SCIENTIFIC REPORTS

Correction: Publisher Correction

OPEN

Co-expression network analysis of toxin-antitoxin loci in *Mycobacterium tuberculosis* reveals key modulators of cellular stress

Received: 20 September 2016
Accepted: 7 June 2017
Published online: 19 July 2017

Amita Gupta[1,3], Balaji Venkataraman[1], Madavan Vasudevan[2] & Kiran Gopinath Bankar[2]

Research on toxin-antitoxin loci (TA loci) is gaining impetus due to their ubiquitous presence in bacterial genomes and their observed roles in stress survival, persistence and drug tolerance. The present study investigates the expression profile of all the seventy-nine TA loci found in *Mycobacterium tuberculosis*. The bacterium was subjected to multiple stress conditions to identify key players of cellular stress response and elucidate a TA-coexpression network. This study provides direct experimental evidence for transcriptional activation of each of the seventy-nine TA loci following mycobacterial exposure to growth-limiting environments clearly establishing TA loci as stress-responsive modules in *M. tuberculosis*. TA locus activation was found to be stress-specific with multiple loci activated in a duration-based response to a particular stress. Conditions resulting in arrest of cellular translation led to greater up-regulation of TA genes suggesting that TA loci have a primary role in arresting translation in the cell. Our study identifed *higBA2* and *vapBC46* as key loci that were activated in all the conditions tested. Besides, *relBE1*, *higBA3*, *vapBC35*, *vapBC22* and *higBA1* were also upregulated in multpile stresses. Certain TA modules exhibited co-activation across multiple conditions suggestive of a common regulatory mechanism.

Mycobacterium tuberculosis, the causative pathogen of the deadly disease tuberculosis, has evolved mechanisms to persist in the human host for long times in a non-replicating and drug-tolerant state, and reactivate at a later time to cause disease. The underlying mechanisms and cellular factors that govern the transition of the bacterium from an active state to latent state are poorly understood[1,2].

Recent studies in *Escherichia coli* and other bacteria point out a prominent role for toxin-antitoxin (TA) systems in stress survival and bacterial persistence[3–7]. TA loci are typically two-component systems that consist of a stable toxin and a relatively unstable antidote of the toxin, the antitoxin, both being encoded as an operon[8]. In most cases, the operon is auto-regulated at the level of transcription by the antitoxin alone and in some cases by the toxin-antitoxin complex[9–11]. Degradation of the labile antitoxin serves as a mechanism for transcriptional induction of TA locus genes as well as for the availability of free toxin protein to act on its cellular target. The most common targets of TA-encoded toxins are translation components; some others have been shown to target proteins belonging to the replication machinery[12–19]. TA-encoded toxins act to rapidly slow down cellular processes, giving bacteria an opportunity to alter their metabolic program and enter into a dormant or non-replicating state and exhibit a persistent or drug-tolerant phenotype[4,6,7,20–22]. Cells unable to adapt to this metabolic slow down initiate a programmed cascade of events leading to cell death[23–25].

Thirty-eight TA loci were initially reported in *M. tuberculosis*[26], however, more are being identified[27]. Presently, *M. tuberculosis* is reported to have 79 TA loci spanning the entire genome[28]. Several reports have been published on the characterization of these loci, identification of the target sites for toxins, structural characterization of some antitoxins, evaluation of their killing effect in *E. coli* and expression under stress[27,29–39]. Stochastic induction of specific TA systems has been proposed to play a role in persistence of *M. tuberculosis* in the host[40–42].

[1]Department of Microbiology, University of Delhi South Campus, Benito Juarez Road, New Delhi, 110021, India. [2]Genome Informatics Research Group, Bionivid Technology Pvt Ltd, Bengaluru, 560043, India. [3]Present address: Department of Biochemistry and Centre for Innovation in Infectious Diseases Research, Education and Training (CIIDRET), University of Delhi South Campus, New Delhi, 110021, India. Correspondence and requests for materials should be addressed to A.G. (email: amitagupta@south.du.ac.in)

Considering the fact that *M. tuberculosis* harbors an unusually high number of TA loci for any bacterial genome and more importantly, significantly higher than other closely related mycobacteria like *M. avium*, *M. bovis* and *M. smegmatis*, it will be useful to analyze the expression profiles of TA genes under different stress conditions thought to mimic the host environment during mycobacterial infection to elucidate their contribution towards the survival ability of this deadly pathogen. While ectopic expression of certain toxins has been shown to inhibit growth of *M. tuberculosis in vitro* and certain TA loci get induced under specific stress[31,32,35,43], a comprehensive profile of genome-wide TA loci of *M. tuberculosis* is lacking. A system-wide screening will help identify specific TA loci differentially expressed under different growth conditions and also shed light on co-regulated pathways/genes that could provide clues to mechanisms for TA activation and regulation.

We have developed a whole-genome microarray platform for *M. tuberculosis* that harbors specific probes for all the 79 TA loci[44]. Prior published microarrays for *M. tuberculosis* did not contain probes for all these 79 TA loci. In the present study, we elucidate TA expression patterns in response to chemical and environmental stress and identify key TA loci that could have potential roles in the pathogenesis of *M. tuberculosis*. This is the first study covering various stress conditions across multiple time points on a single platform with key emphasis on genome-wide TA loci of *M. tuberculosis*.

Results

Expression profiling of TA loci in *M. tuberculosis*. TA loci identified in various bacterial genomes are grouped into families based on sequence homology and biochemical properties[26]. *M. tuberculosis* H37Rv genome harbours 79 TA loci spanning the entire genome (Fig. 1) of which 68 loci have been assigned to the existing TA families. There are three *higBA* loci, ten *mazEF* loci, two *parDE* loci, three *relBE* loci, and fifty *vapBC* loci. The remaining 11 loci (*ucAT*) are uncharacterised and yet to be assigned to existing/novel TA families.

Using a recently described *M. tuberculosis* microarray covering all these 79 TA loci[44], we obtained the expression profile of *M. tuberculosis* H37Rv after subjecting it to various stresses including chemical (drug) stress and environment stress (nutrient starvation and low pH). The four frontline drugs that comprise TB chemotherapy namely Rifampicin (RIF), Isoniazid (INH), Ethambutol (ETH) and Streptomycin (STR) were used in this study to understand changes in expression pattern of TA loci in response to drug administration to the bacteria. Low pH shift was used to mimic environment of mycobacteria in the phagosomal compartment of the host macrophage and starvation (STRV) was used to mimic the nutrient limitation encountered by the bacterium in the host. *M. tuberculosis* was subjected to these stresses and samples at multiple time points were used for expression studies. Quantitative RT-PCR was performed to check expression of selected marker genes and validate the cultures for stress exposure. These marker genes were selected based on published literature[45,46]. The fold change obtained for various genes correlated with published data for different conditions (data not shown). Some of these conditions have been used previously to define the transcriptome of *M. tuberculosis* by Boshoff *et al.*[45]. They have analysed the expression profile of M. tuberculosis H37Rv under different growth conditions in culture. However, their microarray design does not contain probes for all the 79 TA loci nor does their analysis focus on the expression of TA loci under different conditions. Our study aims to address this gap in existing knowledge by providing data and its analysis for all the 79 TA loci.

After transcriptional profiling of all the samples representing eighteen stress conditions, the data obtained was analysed for differentially expressed genes. As shown in Fig. 1, each of the 79 TA locus exhibits differential expression in *M. tuberculosis* in response to one or more stress conditions studied here, signifying the need of the cell to alter the expression of TA genes in response to stress. Further, most genes have altered expression across multiple stress conditions. However, no one gene is expressed under all the conditions tested. Even members from within the same TA family are differentially expressed under different set of conditions. This clearly suggests a stress-specific expression of TA genes. *higBA*1, *higBA*2, *higBA*3, *mazEF*1, *mazEF*6, *mazEF*7, *parD*1, *parD*2, *relBE*3, *vapBC*5, *vapBC*6, *vapBC*14 and *vapBC*21 loci had differential expression of their component genes in at least 50% of the stress conditions studied. Some of the uncharacterised TA loci, namely *ucAT*2, *ucAT*9 and *ucAT*11 were also expressed under multiple stress conditions. It should be noted that these 158 toxin and antitoxin genes out of an approximately 4000 total genes in the mycobacterial genome comprise 4% of the coding capacity of the bacterium and belong to a single stimulus-responsive system, the TA system. This accumulation and conservation of TA loci in large numbers uniformly across the genome and their induction in response to varied environment changes is clearly indicative of their role in increasing the pathogenic fitness of mycobacteria and contributing to its ability to survive in different niches in the host. This also emphasises the need for maintenance of TA loci in a bacterial genome and their ubiquitous presence across the bacterial kingdom.

Stress-induced differential expression of TA loci in *M. tuberculosis*. Variation in copy number of expressed transcripts leads to differences in sensitivity of detection in a microarray platform. In order to comprehensively delineate the differentially expressed TA genes in a sensitive manner, we analyzed the data with variable Fold Change (FC) cut-off at 5% confidence level. The total number of differentially expressed TA genes increased with the duration of the stress for each of the conditions (Fig. 2), suggestive of their essential and growing requirement in stress response. The greatest up-regulation of TA genes was observed in response to STR and nutrient starvation followed by RIF and INH treatments. Shift to low pH resulted in more downregulation of TA genes than upregulation. The number of differentially expressed TA genes reduced when the cutoff was raised from 1.5 to 2.0, however, greater than 50% TA genes were still differentially expressed (Supplementary Table S1). The expression pattern at 1.5 FC and 2.0 FC followed a similar trend (Fig. 2), indicating sensitivity of detection of the microarray platform. Moreover, though the number of genes was higher at lower Fold Change as expected, the TA

Sr.No.	TA LOCI	TA TYPE	TOXIN	Rv NUMBER	START	END	ANTITOXIN	Rv NUMBER	START	END	TOXIN	ANTITOXIN
1	HigBA1	II	HigB1	Rv1955	2201719	2202096	HigA1	Rv1956	2202138	2202587	6	8
2	HigBA2	II	HigB2	Rv2022c	2267119	2267724	HigA2	Rv2021c	2266805	2267110	7	4
3	HigBA3	II	HigB3	Rv3182	3550374	3550718	HigA3	Rv3183	3550715	3551044	8	5
4	MazEF1	II	MazF1	Rv0456A	547076	547357	MazE1	Rv0456B	547344	547517	5	9
5	MazEF10	II	MazF10	Rv0299	363476	363778	MazE10	Rv0298	363252	363479	4	4
6	MazEF2	II	MazF2	Rv0659c	754685	754993	MazE2	Rv0660c	754980	755225	1	3
7	MazEF3	II	MazF3	Rv1102c	1230660	1230971	MazE3	Rv1103c	1230971	1231291	3	3
8	MazEF4	II	MazF4	Rv1495	1686570	1686887	MazE4	Rv1494	1686271	1686573	7	4
9	MazEF5	II	MazF5	Rv1942c	2194644	2194973	MazE5	Rv1943c	2194970	2195347	1	4
10	MazEF6	II	MazF6	Rv1991c	2234305	2234649	MazE6	Rv1991A	2234643	2234891	8	6
11	MazEF7	II	MazF7	Rv2063A	2321057	2321467	MazE7	Rv2063	2320831	2321064	5	8
12	MazEF8	II	MazF8	Rv2274c	2546488	2546805	MazE8	Rv2274A	2546839	2547087	5	5
13	MazEF9	II	MazF9	Rv2801c	3110167	3110523	MazE9	Rv2801A	3110507	3110737	4	3
14	ParDE1	II	ParE1	Rv1959c	2203681	2203977	ParD1	Rv1960c	2203974	2204225	8	2
15	ParDE2	II	ParE2	Rv2142c	2402193	2402510	ParD2	Rv2142A	2402507	2402722	8	1
16	RelBE1	II	RelE1	Rv1246c	1388685	1388978	RelB1	Rv1247c	1388975	1389244	2	5
17	RelBE2	II	RelE2	Rv2866	3177822	3178085	RelB2	Rv2865	3177537	3177818	5	2
18	RelBE3	II	RelE3	Rv3358	3771045	3771302	RelB3	Rv3357	3770773	3771048	5	9
19	VapBC1	II	VapC1	Rv0065	71821	72222	VapB1	Rv0064A	71589	71828	1	3
20	VapBC10	II	VapC10	Rv1397c	1574112	1574513	VapB10	Rv1398c	1574510	1574767	7	5
21	VapBC11	II	VapC11	Rv1561	1764979	1765383	VapB11	Rv1560	1764755	1764973	3	6
22	VapBC12	II	VapC12	Rv1720c	1947030	1947419	VapB12	Rv1721c	1947416	1947643	7	2
23	VapBC13	II	VapC13	Rv1838c	2087257	2087652	VapB13	Rv1839c	2087649	2087912	7	5
24	VapBC14	II	VapC14	Rv1953	2200938	2201249	VapB14	Rv1952	2200726	2200941	4	8
25	VapBC15	II	VapC15	Rv2010	2258273	2258671	VapB15	Rv2009	2258030	2258272	4	3
26	VapBC16	II	VapC16	Rv2231A	2505736	2506161	VapB16	Rv2231B	2506207	2506383	5	4
27	VapBC17	II	VapC17	Rv2527	2851315	2851716	VapB17	Rv2526	2851091	2851318	3	6
28	VapBC18	II	VapC18	Rv2546	2868154	2868567	VapB18	Rv2545	2867783	2868061	5	6
29	VapBC19	II	VapC19	Rv2548	2868860	2869237	VapB19	Rv2547	2868606	2868863	4	5
30	VapBC2	II	VapC2	Rv0301	364044	364469	VapB2	Rv0300	363826	364047	1	1
31	VapBC20	II	VapC20	Rv2549c	2869727	2870122	VapB20	Rv2550c	2870119	2870364	4	4
32	VapBC21	II	VapC21	Rv2757c	3070170	3070586	VapB21	Rv2758c	3070583	3070849	3	9
33	VapBC22	II	VapC22	Rv2829c	3136620	3137012	VapB22	Rv2830c	3137009	3137224	2	3
34	VapBC23	II	VapC23	Rv2863	3174992	3175372	VapB23	Rv2862A	3174747	3174995	2	3
35	VapBC24	II	VapC24	Rv0240	289345	289782	VapB24	Rv0239	289104	289337	5	4
36	VapBC25	II	VapC25	Rv0277c	332708	333136	VapB25	Rv0277A	333160	333417	1	2
37	VapBC26	II	VapC26	Rv0582	677922	678329	VapB26	Rv0581	677710	677925	4	2
38	VapBC27	II	VapC27	Rv0598c	697154	697567	VapB27	Rv0599c	697564	697800	5	5
39	VapBC28	II	VapC28	Rv0609	703486	703887	VapB28	Rv0608	703244	703489	5	5
40	VapBC29	II	VapC29	Rv0617	711006	711407	VapB29	Rv0616A	710782	711009	1	7
41	VapBC3	II	VapC3	Rv0549c	640228	640641	VapB3	Rv0550c	640638	640904	6	4
42	VapBC30	II	VapC30	Rv0624	716664	717059	VapB30	Rv0623	716410	716664	6	7
43	VapBC31	II	VapC31	Rv0749	841228	841656	VapB31	Rv0748	840947	841204	4	5
44	VapBC32	II	VapC32	Rv1114	1239610	1239984	VapB32	Rv1113	1239416	1239613	2	3
45	VapBC33	II	VapC33	Rv1242	1384535	1384966	VapB33	Rv1241	1384278	1384538	5	3
46	VapBC34	II	VapC34	Rv1741	1967917	1968165	VapB34	Rv1740	1967705	1967917	3	3
47	VapBC35	II	VapC35	Rv1962c	2204866	2205273	VapB35	Rv1962A	2205277	2205549	6	3
48	VapBC36	II	VapC36	Rv1982c	2225413	2225832	VapB36	Rv1982A	2225841	2226101	5	4
49	VapBC37	II	VapC37	Rv2103c	2364086	2364520	VapB37	Rv2104c	2364527	2364781	5	6
50	VapBC38	II	VapC38	Rv2494	2808310	2808735	VapB38	Rv2493	2808083	2808304	4	5
51	VapBC39	II	VapC39	Rv2530c	2854267	2854686	VapB39	Rv2530A	2854683	2854907	1	3
52	VapBC4	II	VapC4	Rv0595c	694839	695231	VapB4	Rv0596c	695228	695485	3	2
53	VapBC40	II	VapC40	Rv2596	2925734	2926138	VapB40	Rv2595	2925492	2925737	4	4
54	VapBC41	II	VapC41	Rv2602	2930344	2930784	VapB41	Rv2601A	2930070	2930357	4	5
55	VapBC42	II	VapC42	Rv2759c	3070875	3071270	VapB42	Rv2760c	3071267	3071536	3	1
56	VapBC43	II	VapC43	Rv2872	3183382	3183825	VapB43	Rv2871	3183138	3183395	4	4
57	VapBC44	II	VapC44	Rv3320c	3707642	3708070	VapB44	Rv3321c	3708074	3708316	6	5
58	VapBC45	II	VapC45	Rv2019	2265989	2266405	VapB45	Rv2018	2265280	2265999	1	3
59	VapBC46	II	VapC46	Rv3384c	3799243	3799635	VapB46	Rv3385c	3799635	3799943	6	5
60	VapBC47	II	VapC47	Rv3408	3826548	3826958	VapB47	Rv3407	3826252	3826551	6	3
61	VapBC48	II	VapC48	Rv3697c	4139805	4140242	VapB48	Rv3697A	4140239	4140463	2	5
62	VapBC49	II	VapC49	Rv3180c	3549254	3549688	VapB49	Rv3181c	3549691	3550143	6	6
63	VapBC5	II	VapC5	Rv0627	718282	718689	VapB5	Rv0626	718025	718285	9	4
64	VapBC50	II	VapC50	Rv3749c	4197628	4198137	VapB50	Rv3750c	4198205	4198597	6	3
65	VapBC6	II	VapC6	Rv0656c	752984	753367	VapB6	Rv0657c	753462	753617	9	12
66	VapBC7	II	VapC7	Rv0661c	755335	755772	VapB7	Rv0662c	755769	756023	5	6
67	VapBC8	II	VapC8	Rv0665	758801	759139	VapB8	Rv0664	758532	758804	5	3
68	VapBC9	II	VapC9	Rv0960	1073545	1073928	VapB9	Rv0959A	1073327	1073548	1	3
69	UCAT1	IV	UCT1	Rv0836c	932279	932932	UCA1	Rv0837c	933003	934031	2	4
70	UCAT2	IV	UCT2	Rv1045	1167673	1168554	UCA2	Rv1044	1167053	1167676	10	6
71	UCAT3	IV	UCT3	Rv2826c	3133709	3134593	UCA3	Rv2827c	3134596	3135483	1	3
72	UCAT4	Uncharacterised	UCT4	Rv0059	63200	63892	UCA4	Rv0060	63909	64967	3	4
73	UCAT5	Uncharacterised	UCT5	Rv0910	1014866	1015300	UCA5	Rv0909	1014681	1014860	3	6
74	UCAT6	Uncharacterised	UCT6	Rv0919	1024684	1025184	UCA6	Rv0918	1024211	1024687	2	3
75	UCAT7	Uncharacterised	UCT7	Rv1546	1747195	1747626	UCA7	Rv1545	1746919	1747146	5	6
76	UCAT8	Uncharacterised	UCT8	Rv1989c	2232739	2233299	UCA8	Rv1990c	2233296	2233637	3	4
77	UCAT9	Uncharacterised	UCT9	Rv2035	2281614	2282102	UCA9	Rv2034	2281294	2281617	9	12
78	UCAT10	Uncharacterised	UCT10	Rv2653c	2976586	2976909	UCA10	Rv2654c	2976989	2977234	5	5
79	UCAT11	Uncharacterised	UCT11	Rv3189	3554642	3555262	UCA11	Rv3188	3554298	3554645	8	9

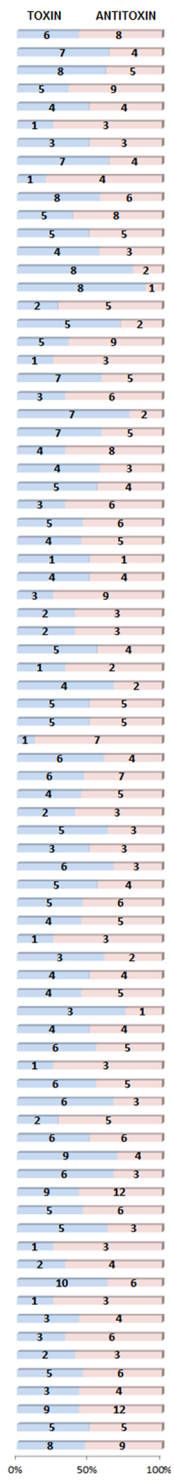

Figure 1. Toxin Antitoxin loci encoded by *Mycobacterium tuberculosis* H37Rv The 79 TA loci present in M. tuberculosis H37Rv genome tabulated with the locus name, gene name for toxin and antitoxin, gene identifier (Rv number), genomic location as Start base position and End base position, orientation in the genome and the type of TA locus. The uncharacterized TA loci are given the nomenclature as ucAT followed by a number for the series. The number in the blue bar indicates the total number of experimental conditions wherein differential expression was observed for the toxin gene and the number in the pink bar indicates the same for the antitoxin gene.

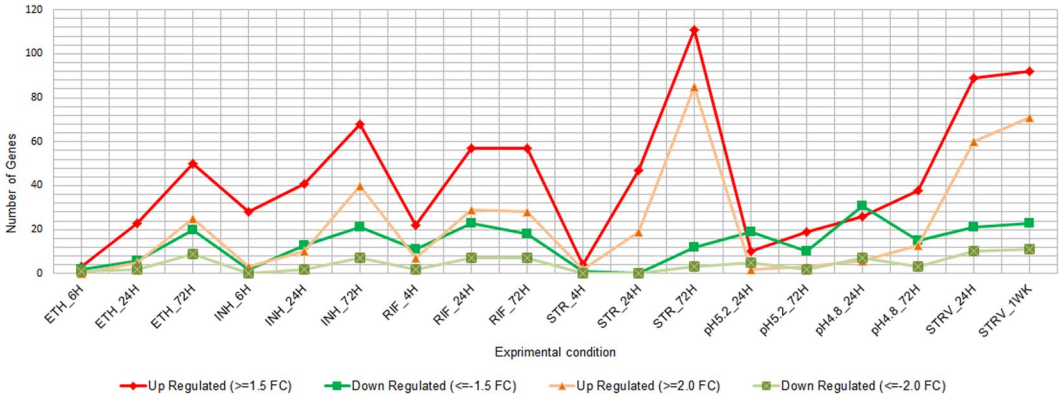

Figure 2. Differentially expressed TA Loci across experimental conditions. Line Graph depicts the number of TA genes that are upregulated and downregulated in each experimental condition at 1.5 and 2.0 fold change. Total number of up and down regulated toxin and antitoxin genes for each condition were plotted using Microsoft excel. The Y-axis indicates total number of toxin and antitoxin genes differentially regulated and X-axis indicates the experimental conditions and time points of the study. Ethambutol (ETH), Isoniazid (INH), Rifampicin (RIF), Streptomycin (STR), Starvation (STRV). 4 H, 6 H, 24 H, 72 H denotes the duration of treatment as 4 hours, 6 hours, 24 hours and 72 hours. 1WK denotes treatment for 1 week.

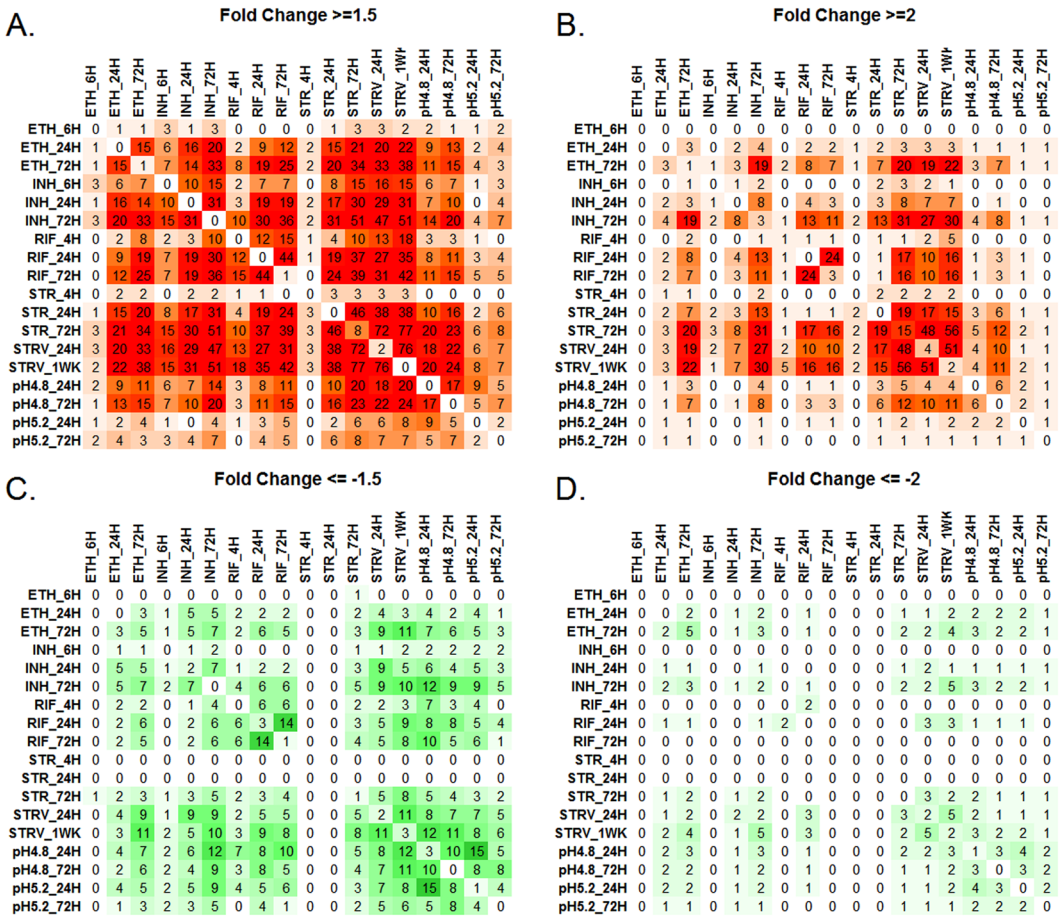

Figure 3. Differential gene expression matrix showing the number of up and down regulated TA genes across the experimental conditions. TA genes up and down regulated at varying sensitivity of detection were subjected to GeneMatrix software which resulted in distribution of up and down regulated genes across 18 conditions profiled. The upregulated genes at 1.5 FC (**A**) and 2.0 FC (**B**) are shown in increasing color of red while the downregulated genes at 1.5 FC (**C**) and 2.0 FC (**D**) are shown in green.

genes identified were truly differentially expressed. The microarray data were validated using qRT-PCR for some of the TA loci. A strong positive correlation (Pearson's correlation coefficient, R = 0.897) was observed between the microarray and qRT-PCR data (Supplementary Fig. S1).

Differentially expressed TA genes unique to a given condition and those expressed across multiple conditions were identified using the matrix shown in Fig. 3. An interactive matrix showing the differentially expressed gene list for each condition is given in Supplementary Fig. S2. At 1.5 FC, 8 TA genes (*vapC*2, *vapC*32, *mazE*4, *mazE*5, *mazE*7, *vapB*38, *vapC*38 and *vapB*19) were uniquely upregulated in response to exposure to Streptomycin for 72 hours (Fig. 3A). These were not common with any other condition tested. Similarly, *vapB*18 was specifically upregulated in response to exposure to Ethambutol for 72 hours and UCT7 in response to Rifampicin for 72 hours. Two TA genes, *vapB*44 and *ucA*5, were specifically upregulated in response to nutrient starvation for 24 hours time period. 50% TA genes were common between Streptomycin and starvation stress, indicating that both the conditions induced similar TA responses in the cell. Several TA genes were found to be common under different stress conditions. Significantly higher numbers of TA genes were upregulated than downregulated under any given condition, supporting the role of TA loci as stress managers in the cell. At 2.0 FC (Fig. 3B and D), more TA genes unique to a given condition were identified. Here also, up-regulation of TA genes in response to streptomycin and nutrient starvation was maximal.

Analysis of the matrix suggests that TA gene transcription is under tight regulation. A marginal change in sensitivity of copy-number of detection by increase in FC from 1.5 to 2.0 leads to a significant drop in the number of differentially expressed TA genes, indicating a likely stringent regulatory control on gene expression. At the same time, a reduction in FC does not substantially increase the number of condition-specific genes, validating that genes identified specific to a given condition are truly specific.

Unsupervised hierarchical cluster analysis of differentially expressed TA loci under different conditions was carried out (Fig. 4). Here again, the TA response clustered nutritional starvation with prolonged exposure to Streptomycin, indicating that the two stress conditions activate similar responses and pathways. The cell wall inhibitors, INH and ETH clustered together while the transcription inhibitor RIF gave a different response. Further, the 72 hours response clustered separately from the shorter duration response signifying the need of the cell to alter the expression of TA genes in response to the duration of stress. The drug–induced response clearly clustered separate from the pH stress-induced response in line with the earlier observation wherein pH was found to significantly down-regulate TA gene expression in contrast to other conditions. The cluster analysis highlights the diversity and division of labour in a biological organisation wherein even a small component like TA system gives a differential, stimulus- specific response.

Impact of frontline TB drugs on transcription of TA loci. The four anti-TB drugs used in this study target different cell components and pathways. We performed an in-depth study of the *M. tuberculosis* transcriptome for cells treated with these drugs for three time points, to capture the primary effect of the drug as well as extended treatment response.

Treatment with Streptomycin had the most profound effect on TA expression. Streptomycin interferes with several steps of protein synthesis, its most conspicuous effect being the stimulation of translational errors and a slowing down of translocation resulting in the production of faulty proteins. A large number of TA loci were differentially regulated in response to this drug. Most loci were upregulated with increased duration of drug exposure (Fig. 4 and Supplementary Table S1). The toxin as well as antitoxin genes were upregulated for all the three *higBA* loci with progressively increasing levels. The toxin partner showed higher transcript levels compared to the cognate antitoxin. *higB*1 toxin showed a 25-fold increase, *higB*2 showed a 23-fold increase and higB3 showed a 10-fold increase in expression levels following exposure of the cell to STR for 72 hours. The toxin component of the uncharacterized TA locus *ucAT*9 showed a 21-fold increase in transcript levels. Both genes comprising *relBE*3, *vapBC*25 and *vapBC*31, *vapBC*36, *vapBC*41, *vapBC*45 and *vapBC*46 loci were also upregulated 2–10 fold at 24 hrs post-drug exposure. At 72 hrs of exposure to STR, 25 loci were upregulated. For some of these loci including *mazEF*5, *mazEF*8, *vapBC*18, *vapBC*20, *vapBC*24 and *vapBC*33, the toxin was upregulated while the antitoxin partner gene showed less or no upregulation.

Rifampicin, another frontline TB drug acts on the mycobacterial RNA polymerase leading to inhibition of transcription. The expression profile of TA loci in response to Rifampicin, across three time points is shown in Fig. 4. Rifampicin exposure induced differential expression of several TA loci. A total of 26 genes were upregulated and 22 genes were downregulated. At 4 hrs post-exposure, minimal changes in expression of TA loci were observed with *vapBC*16, *vapBC*23 and *vapBC*49 showing a 2–4 fold upregulation. However, by 24 hrs of drug exposure, a substantial number of TA genes were differentially expressed with several of them being upregulated 2–4 fold. *higBA*3, *mazEF*1, *mazEF*6, *mazEF*9, *parDE*2, *relBE*1, *relBE*2, *ucAT*1, *ucAT*2, *ucAT*10, *ucAT*11, *vapBC*1, *vapBC*3, *vapBC*4, *vapBC*8, *vapBC*11, *vapBC*13, *vapBC*16 and *vapBC*39 showed up-regulation of both partners at 24 hrs. *vapC*11, *vapC*24, and *vapC*40 toxins were preferentially upregulated compared to their antitoxin counterparts. *vapBC*10, *vapBC*14, *vapBC*22, *vapBC*27, *vapBC*44, *vapBC*47 and *vapBC*50 were downregulated 4–10 fold across all time-points. In an earlier study, Singh *et al.*[36] have also reported significant upregulation of *relB*1 and *relB*2 antitoxins following exposure to Rifampicin. Their results corroborate with our observations.

The changes in expression profiles of TA loci in response to Ethambutol and Isoniazid, both of which target the cell wall system, were analyzed. While there was no significant change in TA gene expression at 6 hours of drug treatment, differential expression was observed 24 and 72 hours post-drug exposure. *vapC*7, *vapB*29, *vapC*30, *vapB*4, *vapC*4, *vapB*43, *vapB*49 and *vapC*49 were upregulated 2 fold in response to Ethambutol exposure for 72 hours while *vapBC*44, *vapC*45 and *vapC*47 were down regulated. While the fold change in expression levels was only 2 fold for most loci, *ucAT*9 showed a 13-fold upregulation for the antitoxin gene and a 5-fold upregulation for the toxin gene, clearly emerging as a locus responsive to ETH exposure. *mazE*6, *mazF*6 and *parD*2 were induced in response to both Ethambutol and Isoniazid. All the three *higBA* loci showed a 2–4 fold upregulation

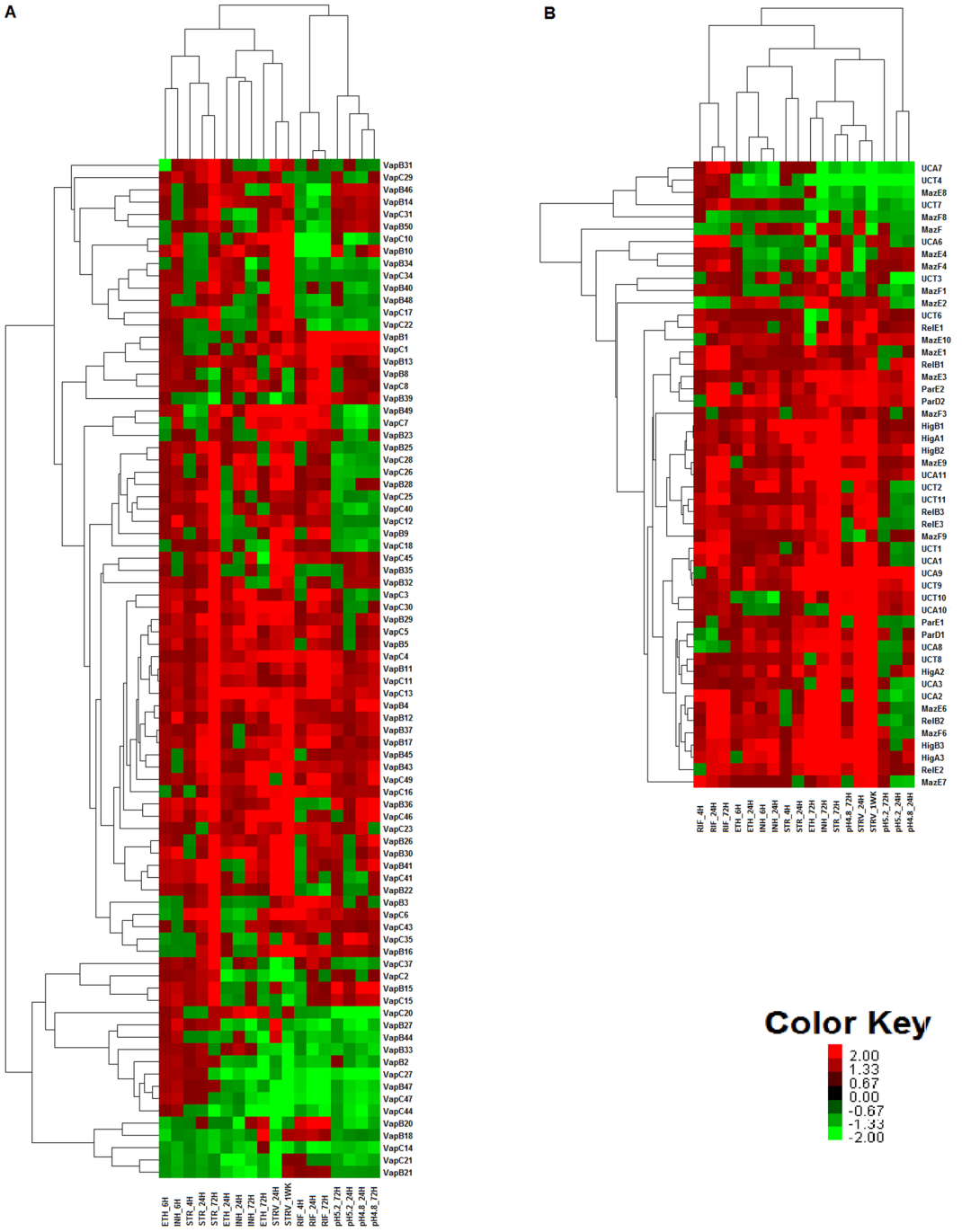

Figure 4. Unsupervised hierarchical clustering analysis of Differentially expressed TA Loci TA genes 1.5 fold up and down regulated along with their fold change were subjected to unsupervised hierarchical clustering. Up regulated genes are in red color gradient and down regulated genes are in green colour gradient. Fold change of 2 was given as a cutoff to render the cluster image to identify patterns of up and down regulated genes.

in response to Isoniazid exposure. *mazEF*2, *mazEF*6, *mazEF*9, *mazEF*10, *relBE*2, *relBE*3, *ucAT*1, *ucAT*2, *ucAT*3, *ucAT*8, *ucAT*9, *ucAT*11, *vapC*3, *vapBC*4, *vapBC*5, *vapBC*7, *vapBC*8, *vapC*13, *vapC*20, *vapC*23, *vapC*26, *vapBC*28, *vapBC*29, *vapBC*30, *vapB*34, *vapBC*41, *vapBC*43, *vapBC*45 and *vapBC*49 were also upregulated 2–5 fold in response to Isoniazid exposure. *ucA*7 and *vapC*27 were downregulated 2–4 fold in response to Isoniazid.

Impact of environmental stress on transcription of TA loci. Nutrient starvation and acidic pH are two stressful environments encountered by mycobacteria in the host. Accordingly, the TA expression profile in response to these stress conditions was studied. We followed the Betts *et al.*, method for starvation studies[47] wherein the early exponential stage *M. tuberculosis* was re-suspended with PBS for starvation and monitored over 24 hrs and 1 week. Starvation led to generalized induction of TA loci, with a large number of TA loci upregulated

A.

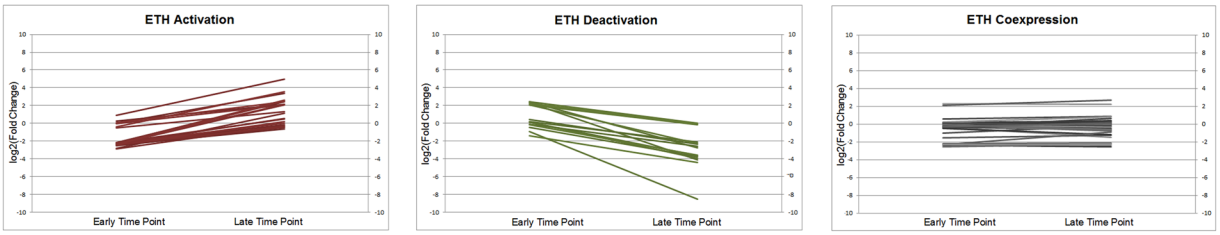

B.

Experimental Condition	Activation	Deactivation	Coexpression
ETH	35	46	77
INH	37	29	92
RIF	42	12	104
STR	100	12	46
STRV	52	27	79
pH4.8	24	4	130
pH5.2	40	10	108

Figure 5. (**A**) Line Graph depicting the approach used to calculate activation and deactivation scores for TA loci (**B**) Number of TA loci that are activated, deactivated and co-expressed in each of the experimental conditions profiled. Fold change of toxin from cognate antitoxin was subtracted in early and late time point. The subtracted scores were subjected to biclustering/K-means clustering using Pearson Uncentered algorithm in GeneSpring Gx v 12.8 to provide 3 clusters of all the 78 TA loci, with clusters representing activation, deactivation and co-expression status. Similar approach was followed for each of the experimental conditions and TA loci activated, deactivated and co-expressed in each condition were identified.

at both 24 hrs and 1 week (Fig. 4 and Supplementary Table S1). Maximal induction was observed for *higBA*1, *higBA*2, *higBA*3, *mazEF*3, *mazEF*6, *mazEF*9, *parDE*1, *parDE*2, *relBE*1, *relBE*2, *relBE*3, *vapBC*4, *vapBC*9, *vapBC*10, *vapBC*12, *vapBC*16, *vapBC*17, *vapBC*22, *vapBC*23, *vapBC*26, *vapBC*28, *vapBC*30, *vapBC*32, *vapBC*34, *vapBC*35, *vapBC*41, *vapBC*45, *vapBC*46, *vapBC*49, *ucAT*1, *ucAT*2, *ucAT*3, *ucAT*8, *ucAT*9, *ucAT*10 and *ucAT*11. As many as twenty-eight loci were upregulated in response to starvation. Most of these TA loci encode translation-inhibiting RNases. Possibly, these toxins when activated in response to starvation, lead to inhibition of translation and selective degradation of mRNA to make nutrients available for survival under stress. *ucAT*9 showed a 36 fold induction after 24 hours of starvation and this increased to more than 100 fold induction after 1 week starvation. Similarly, *ucAT*1, *higBA*1, *higBA*2, and *higBA*3 showed a 10–18 fold upregulation. For *higBA*1, *higBA*2, *relBE*2, *ucAT*10, *vapBC*1, *vapBC*6, *vapBC*7, *vapBC*34, *vapBC*35, *vapBC*45 loci, the toxin was upregulated to higher levels compared to the antitoxin partner.

In contrast to starvation that led to generalized up-regulation of TA loci, low pH exposure led to down-regulation of TA genes (Fig. 4). The effect was more pronounced at pH 4.8 vis-à-vis pH 5.2. *higBA*2, *vapBC*1, *vapBC*4, *vapBC*15, *ucAT*10 and *ucAT*9 showed 2–5 fold upregulation following exposure to pH 4.8 for 72 hours. *mazEF*8, *ucAT*2, *ucAT*3, *ucAT*4, *ucAT*7, *vapC*7, *vapC*9, *vapC*20, *vapC*21, *vapBC*27, *vapBC*47 and *vapB*49, showed 2-fold down regulation at both pH 5.2 and pH 4.8.

TA regulatory network under stress. The TA transcriptome data showed that in spite of being expressed as an operon, the antitoxin and toxin levels for a given TA locus were not same across all conditions and time points (Supplementary Table S1). Based on this, we calculated the activation/deactivation scores for TA loci as described in methods to determine condition-specific TA responses. This is diagrammatically represented in Fig. 5A. If the median fold change difference between toxin transcript and antitoxin transcript level increased with duration of stress, it was designated as TA activation representing a net increase in toxin transcript vis-à-vis antitoxin transcript. The reverse was designated as TA deactivation. STR and STRV led to activation of majority of TA loci. Bi-clustering and Hierarchical clustering of the profiles based on these scores also showed a pattern of condition-based clustering (Fig. 6). The STR and STRV response was highly similar and clustered together. Both stresses led to activation of common TA loci. Nutrient starvation has been shown to cause metabolic slow-down in cells to economize on available resources, which results in arrest of translation, a phenomenon similar to Streptomycin action. The common response in the two conditions and the greater up-regulation of TA genes suggests that TA loci have a primary role in arresting translation in the cell. This is in line with the suggested mechanisms of TA loci wherein several of them are known to be mRNA interferases. The profile in response to RIF was completely in contrast to the STR and STRV response. RIF exposure led to deactivation of almost 90% TA loci. The cell wall inhibitor antibiotics, namely INH and ETH clustered separately and led to activation of some common and other different TA loci. Shift to a lower pH of 5.2 did not cause substantial changes in TA loci regulation; however, shift to pH 4.8 led to a dramatic increase in the number of activated TA loci giving a response similar to STR and STRV response. This suggests that the TA activation-deactivation response is stress-related.

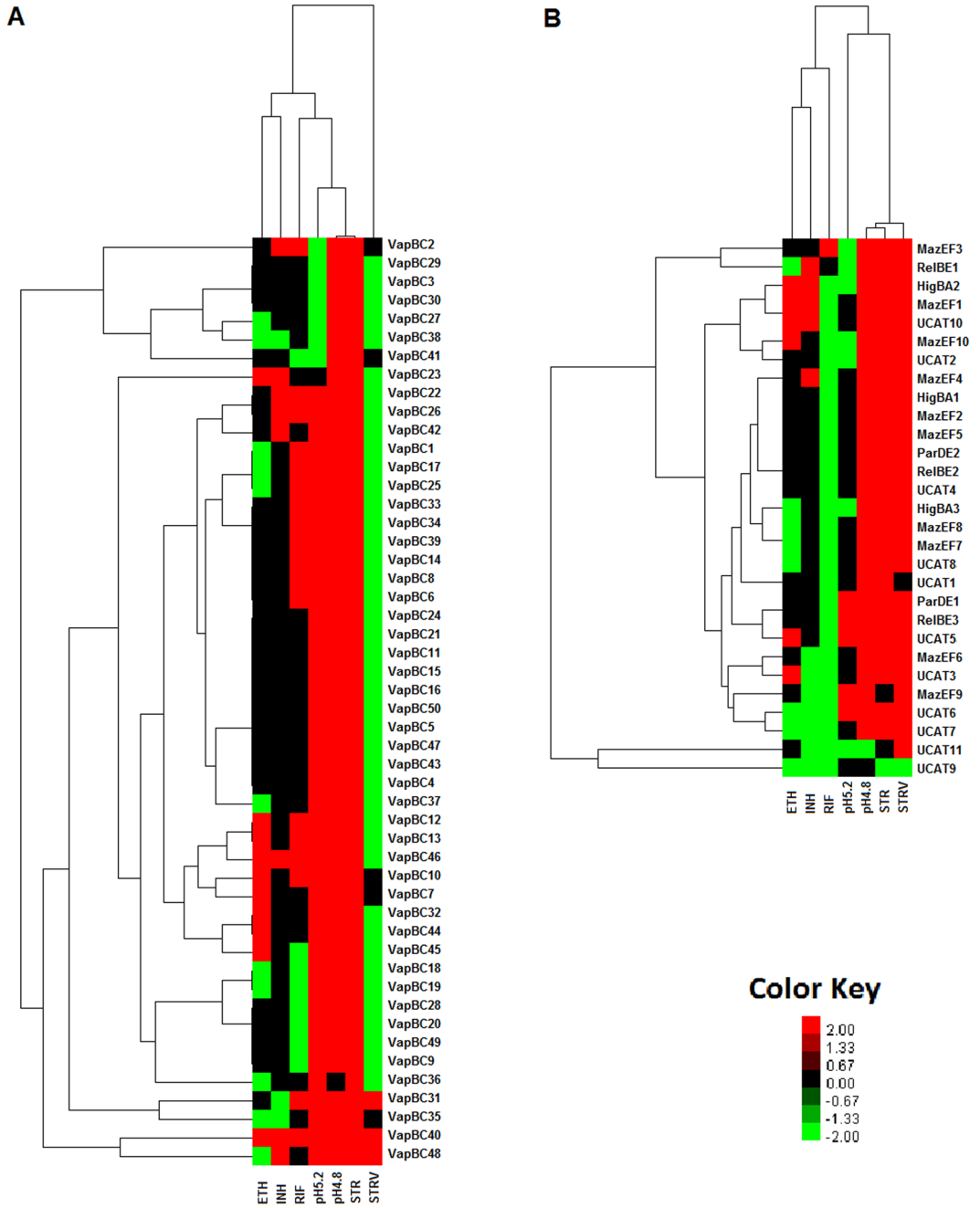

Figure 6. Unsupervised hierarchical clustering analysis of TA loci based on their activation and deactivation status in response to stress. All the 79 TA loci with their activation-deactivation and co-expression status defined as 2 for activation, −2 for deactivation and 0 for co-expression were subjected to unsupervised hierarchical clustering using Cluster 3.0 software by applying Pearson Uncentered algorithm with average linkage rule. The resultant cluster file was imported into Java Treeview software to visualize the cluster. Activated TA loci are in red color gradient and Deactivated TA loci are in green color gradient. A score of 2 was given as a cutoff to render the cluster image to identify patterns of activation and deactivation of TA loci across conditions profiled.

Different chemical and environment stress trigger varied responses in the cell and lead to activation of specific sets of TA loci, which might be helping bacteria overcome the stress.

Cluster analysis further showed that certain TA loci were co-activated under different stress conditions. *higBA1, mazEF2, mazEF5, parDE2, relBE2* and *ucAT4* were always activated and deactivated under same conditions indicating that they had common regulatory mechanisms. Similarly, *mazEF7, mazEF8* and *ucAT8* were co-regulated and clustered together. ucAT9 and ucAT11 showed a completely different pattern of regulation and formed a separate cluster from the other loci. Perhaps different sets of transcription factors responded to different stimuli and regulated different groups of TA loci.

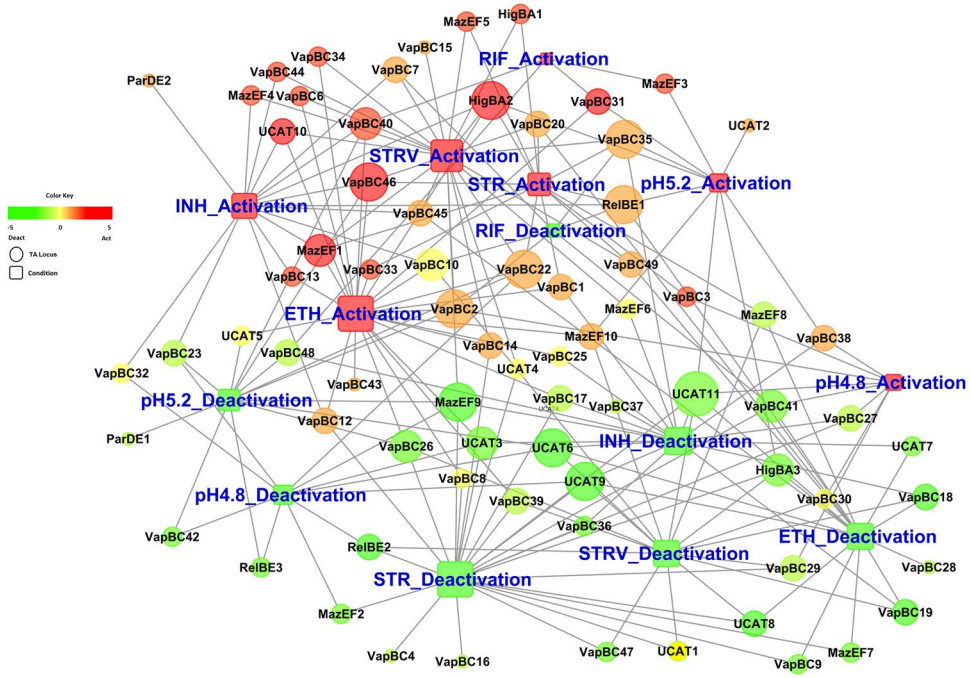

Figure 7. Biological Network of TA loci. Condition-based list of TA loci activated and deactivated was provided to BridgeIsland software. This software identifies the nodes and edges that come together to form a network of connections that could be representative of the TA gene regulation. The nodes (TA loci) are colored based on the activation and deactivation levels with activation being colored in red gradient and deactivation being colored in green gradient and co-expression colored in yellow gradient. The nodes are sized based on their connectivity scores with larger the size indicating a TA is activated/deactivated in as many conditions profiled.

The data were further plotted to create a TA activation-deactivation network (Fig. 7). All the TA loci were mapped based on their activation and deactivation scores with the intensity of the color correlating to the scores and the diameter of the circle corresponding to the number of conditions in which activation-deactivation was observed. As shown, there is a clear grouping of loci that are activated from those that are deactivated. *vapBC40*, *higBA*2 and *vapBC*46 were highly activated in all the conditions except low pH 5.2. *relBE*1, *vapBC*35, *vapBC*22, *vapBC*2 were also upregulated in 4 out of 6 stresses, however, the activation score was less than that for *higBA*2 and *vapBC*46. *mazEF*9 was activated in 2 conditions and deactivated in 4 conditions. ucAT11 was deactivated in all the 6 conditions studied. Other loci including *vapBC*41, ucAT6, ucAT9 and *higBA*3 were downregulated in 5 out of the 6 conditions. *vapBC*13 was uniquely activated in response to INH and ETH treatment while *parDE*2 was activated under INH stress. Several other loci were activated or deactivated under one or more conditions tested. Most loci exhibited an activation or deactivation trend across all conditions. Only 9 out of the 79 TA loci showed a mixed trend with activation under some conditions and deactivation in other conditions.

The TA activation-deactivation network clearly points out a stress-responsive activation of specific TA loci and a division of labour amongst the large number of loci. Not all TA loci are activated in response to a stress and every stress does not activate the same set of TA loci. While the cellular functions are not understood for a greater number of these loci, this data clearly indicates that the large number of TA loci maintained in mycobacterial genome does not simply comprise of pseudo genes or redundancy in gene function. Rather, these loci encode functional proteins expressed in response to specific stimulus.

Expression of cellular proteases and nucleases under stress. According to the existing model, TA loci are activated during stress by degradation of antitoxin partner by cellular proteases enabling the free toxin to exert its effect[48–51]. In this context, we checked the expression pattern of 26 annotated mycobacterial proteases under stress. As shown in Fig. 8A, several proteases were upregulated during STR and STRV stress. The Clp family proteases that have been shown to cause antitoxin degradation in several bacteria[48,50] were found to be upregulated in our study indicating that they may play similar roles in *Mycobacterium tuberculosis*. The protease activation pattern aptly correlates with the TA activation data wherein, many TA loci were activated during STR and STRV. Two potential proteases, Rv1577c and Rv2651c were found to be upregulated under all stress conditions except INH stress. Six of the nine putative RNases of *M. tuberculosis* were also activated under one or more stress conditions (Fig. 8B). Again, maximum activation was observed under STRV and low pH stress. Further studies on these gene products can elucidate their possible roles in TA activation during stress in mycobacteria.

Discussion

This paper is the first report providing experimental data on the expression profiles of all the seventy-nine chromosomally encoded toxin-antitoxin loci in *M. tuberculosis*. The data generated herein is used to understand

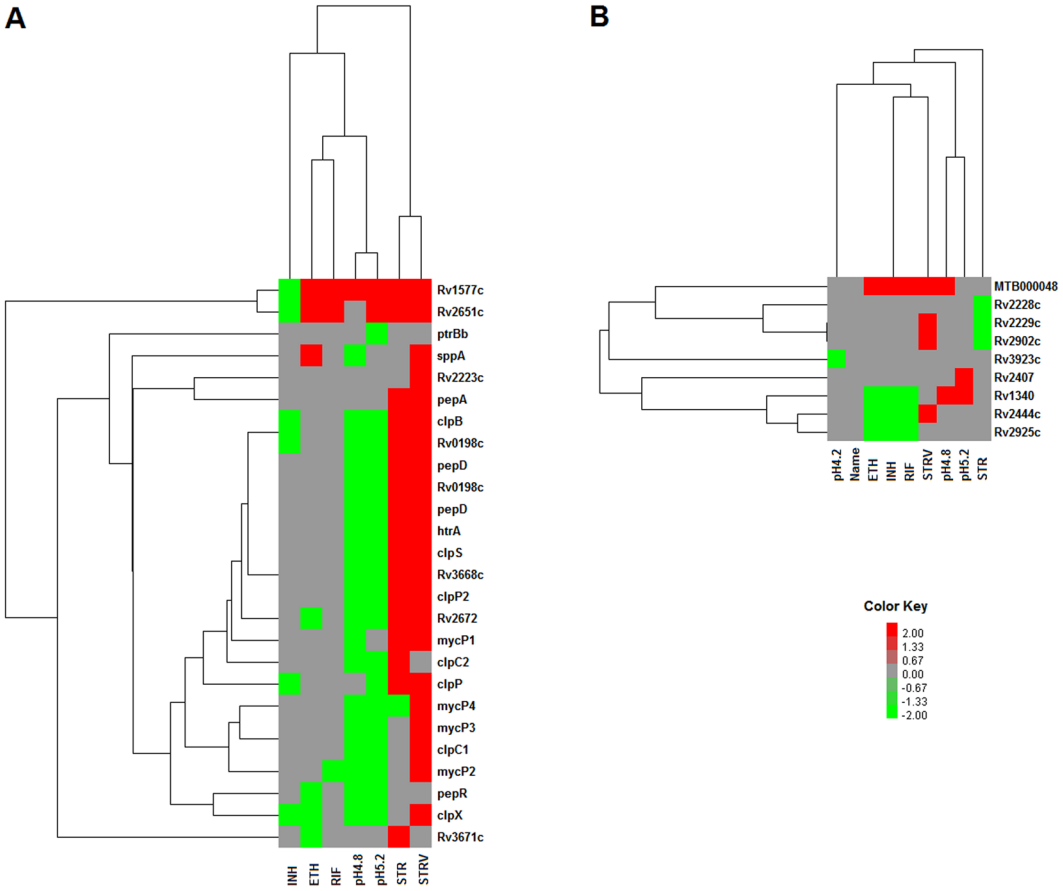

Figure 8. (**A**) Unsupervised hierarchical clustering analysis of protease genes based on their activation and deactivation status in response to stress. (**B**) Unsupervised hierarchical clustering analysis of nuclease genes based on their activation and deactivation status in response to stress Fold change of genes in late time point was subtracted from early time point to calculate the activation deactivation score. The cluster was created as described for Figs 5 and 6.

activation and deactivation of TA loci in a time-dependent manner in response to environmental and chemical stresses and identify key players in cellular stress.

TA loci are being identified in many genomes and in greater numbers in each genome. This definitely raises curiosity about their possible roles in bacterial survival and persistence. *M. tuberculosis* supersedes most other bacteria for the number of TA loci it harbors in its genome. Consequently, there has been a continuing effort investigating TA loci in *M. tuberculosis*. Previous work from our lab and other groups has demonstrated killing activity of mycobacterial TA loci in heterologous hosts and native system[27,30,31,35,39,43,52–57]. Further, it has been shown that TA locus deletion strains of mycobacteria exhibit growth defective phenotype[58].

To understand the conditions under which TA loci get induced in *M. tuberculosis*, we performed a genome-wide study and identified some key TA loci that are activated in response to chemical and/or environmental stress in *M. tuberculosis*. It is important to note here that all the 79 TA loci encoding 158 proteins in this study show specific differential regulation in one or more stress conditions. No random selection of 158 genes for any genome is expected to show such behavior supporting the conclusion that TA genes are stress-responsive and are helping bacteria tide over unfavorable conditions.

Our results corroborate with previous reports on expression of TA genes in *M. tuberculosis*[31,36,59]. Individual TA loci have been studied and shown to be induced during hypoxia, nitrogen limitation, starvation and drug exposure[27,31,32]. The *vapBC* locus in *M. smegmatis* has been implicated as playing a role in regulation of metabolic flux[60]. Singh *et al.* have also shown increased survival of *relE* overexpressing cells during drug treatment[36]. Several TA loci were identified to be upregulated in *M. tuberculosis* drug-tolerant persister population[61]. While all these studies have provided knowledge on TA loci and their activity, a comprehensive analysis of all the loci on a single platform was lacking. A genome-wide analysis of TA loci in this study has filled this gap and enabled identification of TA loci responsive to varied stress conditions. *higBA*2 and *vapBC*46 emerge as key players getting upregulated to high levels in response to chemical as well as nutritional stress. *mazEF*1, *vapBC*31, *ucAT*10 also are activated under both kinds of stress though to lesser levels. *higBA*1 and *mazEF*5 get activated in response to nutritional starvation and streptomycin treatment. Several of the TA loci identified to be activated under stress, like *mazEF*1, *vapBC*31, *higBA*1 and *mazEF*5 have been shown to have killing activity across mycobacterial species and even in heterologous systems[27,30,36]. All the three *higBA* loci in *M. tuberculosis* have been studied here and

higBA2 appears to be another important locus besides *higBA1* that has been the focus of earlier studies[56]. Many of the hitherto uncharacterised TA loci, *ucAT*11, *ucAT*6, *ucAT*9 show strong deactivation in response to both chemical and nutritional stress. Although individual deletions of TA genes have not been found to impair bacterial survival in a mouse infection model[36], it does not rule out a role for TA loci in *M. tuberculosis* infection and survival in the human host.

Inhibition of translation is a key event in stress response and development of persistence and drug-tolerant phenotype in *E. coli*. The HigB, RelE, MazF and VapC toxins from diverse bacterial species have been identified to be mRNA interferases that cleave cellular RNA at specific sequences[15,38,43,62]. Transcriptomic analyis of *E. coli* persister cells reveals over-expression of TA modules and their encoded mRNA interferases[5,6]. Antibiotic and starvation stress has also been linked with expression of mRNA interferases[3]. The transcriptional upregulation of TA loci as observed in our study suggests a similar mechanism of translation shut-down operating in mycobacteria to impart a survival advantage to the bacteria under antibiotic pressure and nutrition deficiency. Stress-induced simultaneous activation of multiple loci would enable a rapid shutdown of cellular machinery and metabolic slowdown leading to a dormant phenotype.

In light of the above observations, TA modules could be essential genes for mycobacteria. At the same time their large number in the mycobacterial genome points towards possibilities of redundancy and pseudogene behaviour. Whole genome screens using transposon libraries have been conducted in *M. tuberculosis* to identify essential genes[63,64]. The screen includes several of the TA genes; however, none of them fall in to the category of essential genes. This is not surprising since knockout of all the ten TA loci in *E. coli* had no phenotype for normal growth and survival. Nonetheless deletion of multiple toxin genes drastically reduced tolerance to antibiotics and the level of persisters[7] suggesting that TA genes provided selective survival advantage to cells under stress. Analysis of a recent essentiality screen data substantiates this observation[65]. Here, TA loci including *higBA1, higBA2, parDE2, VapBC6, VapBC13* and *UCAT3* are listed to confer growth advantage to mycobacteria. In our study also, *higBA1*, *higBA2* and *parDE2* are key TA modules. Essentiality of a gene for survival of the organism is dictated by the environment and a gene which is non-essential under normal growth conditions may become important under adverse conditions. TA loci appear to be one such set of genes which maybe non-essential under favourable growth conditions but confer survival advantage to the bacteria under unfavourable, stress conditions as are encountered in the human host.

Another important finding that emerges from this study is that even though the TA locus is an operon and its mRNA codes for both the toxin and antitoxin partner, the actual mRNA levels for the toxin and antitoxin genes are different. This has been reported in earlier publications[32,36]. Singh *et al*. have shown higher levels of toxin RNA compared to cognate antitoxin RNA for the three RelBE loci in lungs of *M. tuberculosis*-infected mice[36]. Korch *et al*. have also shown differences in levels of toxin and antitoxin RNA for the RelBE loci in *M. tuberculosis* when grown under hypoxic and starvation conditions[32]. The differential level of toxin and antitoxin mRNA in the cell at a given time could be a mechanism for regulating the ratio of antitoxin to toxin in the cell. Differential degradation of polycistronic RNA has been shown to determine differential expression of genes within an operon in several prokaryotic systems including *E. coli*, *Salmonella typhimurium* and *Rhodobacter capsulatus*[66–72]; however, the mechanisms involved are poorly understood. Degradation has been found to be RNaseE-dependent[70], mRNA secondary structure based[72,73] and small regulatory RNA (sRNA) induced[74]. Differential dosage of transcripts for *kis* and *kid* of the *parD* stability system of plasmid R1 has been shown to be a consequence of limited degradation of the polycistronic *par*D mRNA[75]. This plasmid addiction system is similar to the chromosomal toxin-antitoxin system. The expression of mycobacterial nucleases and proteases is also upregulated especially under STR and STRV stress. Protease-mediated degradation of antitoxins is well studied in *E. coli* and *Streptococcus aureus*[48–51] and has been shown to contribute to increased toxin activity with enhanced drug resistance and persistence[76]. Similar studies in *M. tuberculosis* will shed light on the relevance of these observations and the role of nucleases and proteases in TA activation.

In summary, the present study provides vital information and clues for further studies on TA members in a genome by giving (i) direct experimental evidence for functionality of a system, (ii) configuration of the system in a genome, (iii) the activeness and responsiveness of a system to stimulus, (iv) a comprehensive analysis of the entire system across multiple time points and conditions, and (v) resolution of the system to identify key players with evidence for a division of labor across the TA system.

Methods

Growth of *M. tuberculosis* and RNA isolation. *M. tuberculosis* H37Rv was grown in Middlebrook 7H9 (Difco, Becton-Dickinson and Co., USA) supplemented with 0.05% Tween 80 and 10% albumin-dextrose-catalase (ADC, Difco, Becton-Dickinson and Co., USA) at 37 °C and 200 rpm, till an OD_{600} of 0.4–0.5. The culture was then split for addition of Isoniazid (isonicotinylhydrazine), Streptomycin and Ethambutol dissolved in autoclaved distilled water at a final concentration of 1 μg/ml and Rifampicin dissolved in ethanol at 0.1 μg/ml. Incubation was continued after addition for different time periods and control cultures (vehicle only) were also grown for same time periods. Cell density was measured as OD_{600} at all time points and CFU assay was performed. To prepare biological replicates for RNA isolation, each culture was independently grown in duplicate. Cells were harvested after 4, 6, 24, and 72 hrs of drug treatment and RNA was isolated. For nutrient starvation, the log phase culture of *M. tuberculosis* (OD_{600} of 0.4–0.5) was pelleted, washed twice with Phosphate Buffer Saline (PBS; 50 mM phosphate buffer, pH 7.4; 150 mM NaCl) containing 0.05% Tween 80, suspended in PBS and grown for 24 hrs and 1 week in tight-capped bottles as standing culture. Untreated culture grown in 7H9 served as control. For pH stress, the log phase culture of mycobacteria was re-suspended in Middlebrook 7H9 media with pH 5.2/pH 4.8 and grown for 24 and 72 hrs at 200 rpm. Control cultures were grown in 7H9 media with pH 6.8. The cells were harvested by centrifugation at 5000 *g* for 5 minutes at 4 °C and used for RNA isolation.

RNA isolation and Quantitative RT-PCR was performed using previously described methods[77].

Microarray processing and data analysis. Using random nucleotide-based T7 promoter primers included in the Low Input Quick Amp WT labelling kit (Agilent Technologies, USA), 25 ng of RNA was amplified and labelled. The labelled cRNA were purified using RNeasy columns (QIAGEN Inc, USA). cRNA yields and specific activities were measured using Nanodrop 2000c spectrophotometer (Thermo Scientific, USA). Microarrays were synthesized using the proprietary non-contact SurePrint Ink-jet technology (Agilent Technologies, USA). The microarray specifications and design have been described earlier[44]. For all arrays, the Gene Expression Hybridization Kit (Agilent Technologies, USA) and recommended protocols were employed. Hybridization and slide processing were done according to the procedure described by Agilent Technologies. Microarray slides were scanned at a resolution of 5 µm using an Agilent Microarray scanner (G2565CA) with scan control software as per the manufacturer's instructions. Raw data obtained were normalized and analyzed as described previously[44]. Probes that showed a 2-fold or higher change with a p value < 0.05 (unpaired Student t-test) were considered to be differentially expressed.

To identify differentially expressed genes that were unique to a given condition and those that were common with other conditions, a matrix was created using GeneMatrix software (Bionivid Technology Pvt Ltd, Bangalore, India). For this, the list of differentially expressed genes in each condition was provided as input to the software that computes all condition vs all condition matrix and identifies genes differentially expressed in one condition and those expressed across multiple conditions. TA genes 1.5 fold up and down regulated along with their fold change were subjected to unsupervised hierarchical clustering using Cluster 3.0 software by applying Pearson Uncentered algorithm with average linkage rule. The resultant cluster file was imported into Java Treeview software to visualize the cluster.

For determination of TA activation levels, the difference in fold change levels of toxin transcript level to antitoxin transcript level for all stress conditions and time points was calculated. If this median fold change difference increased from an early time point to a later time point under stress, it was designated as TA activation while if it decreased from an early to a later time point, it was designated as TA deactivation. If the difference remained equal to 1, it was designated co-expression. This model was used to calculate activation/deactivation scores and determine the pattern of TA response to a particular stress condition. Bi-clustering and Hierarchical clustering using Pearson uncentered algorithm with average linkage rule was used to identify the list of TA loci that were activated and deactivated. To construct the regulatory network for TA loci, the list of activated and deactivated TA loci along with the condition in which it was measured were provided as input to BridgeIsland software (Bionivid Technology Pvt Ltd, India). BridgeIsland software identifies the connecting nodes and edges from the raw input and derives the list of connections (TA– > Activation/Deactivation– > Condition) enriched in the overall experiment. Further, this information is provided as an input to CytoScape V 2.8.2 (NIGMS, NIH, USA) to visualize the network. Force-directed spring-embedded layout algorithm was applied to the network and nodes were sized based on their connectivity score with larger nodes bearing the highest score.

References

1. Gomez, J. E. & McKinney, J. D. M. tuberculosis persistence, latency, and drug tolerance. *Tuberculosis (Edinb)* **84**, 29–44 (2004).
2. Stewart, G. R., Robertson, B. D. & Young, D. B. Tuberculosis: a problem with persistence. *Nature reviews. Microbiology* **1**, 97–105, doi:10.1038/nrmicro749 (2003).
3. Christensen, S. K., Mikkelsen, M., Pedersen, K. & Gerdes, K. RelE, a global inhibitor of translation, is activated during nutritional stress. *Proceedings of the National Academy of Sciences of the United States of America* **98**, 14328–14333 (2001).
4. Fu, Z., Tamber, S., Memmi, G., Donegan, N. P. & Cheung, A. L. Overexpression of MazFsa in Staphylococcus aureus induces bacteriostasis by selectively targeting mRNAs for cleavage. *Journal of bacteriology* **191**, 2051–2059, doi:10.1128/JB.00907-08 (2009).
5. Gerdes, K., Christensen, S. K. & Lobner-Olesen, A. Prokaryotic toxin-antitoxin stress response loci. *Nature reviews. Microbiology* **3**, 371–382, doi:10.1038/nrmicro1147 (2005).
6. Keren, I., Shah, D., Spoering, A., Kaldalu, N. & Lewis, K. Specialized persister cells and the mechanism of multidrug tolerance in Escherichia coli. *Journal of bacteriology* **186**, 8172–8180, doi:10.1128/JB.186.24.8172-8180.2004 (2004).
7. Maisonneuve, E., Shakespeare, L. J., Jorgensen, M. G. & Gerdes, K. Bacterial persistence by RNA endonucleases. *Proceedings of the National Academy of Sciences of the United States of America* **108**, 13206–13211, doi:10.1073/pnas.1100186108 (2011).
8. Engelberg-Kulka, H. & Glaser, G. Addiction modules and programmed cell death and antideath in bacterial cultures. *Annual review of microbiology* **53**, 43–70 (1999).
9. de Feyter, R., Wallace, C. & Lane, D. Autoregulation of the ccd operon in the F plasmid. *Molecular & general genetics: MGG* **218**, 481–486 (1989).
10. Magnuson, R., Lehnherr, H., Mukhopadhyay, G. & Yarmolinsky, M. B. Autoregulation of the plasmid addiction operon of bacteriophage P1. *The Journal of biological chemistry* **271**, 18705–18710 (1996).
11. Magnuson, R. & Yarmolinsky, M. B. Corepression of the P1 addiction operon by Phd and Doc. *Journal of bacteriology* **180**, 6342–6351 (1998).
12. Bernard, P. & Couturier, M. Cell killing by the F plasmid CcdB protein involves poisoning of DNA-topoisomerase II complexes. *Journal of molecular biology* **226**, 735–745 (1992).
13. Christensen, S. K., Pedersen, K., Hansen, F. G. & Gerdes, K. Toxin-antitoxin loci as stress-response-elements: ChpAK/MazF and ChpBK cleave translated RNAs and are counteracted by tmRNA. *Journal of molecular biology* **332**, 809–819 (2003).
14. Critchlow, S. E. *et al.* The interaction of the F plasmid killer protein, CcdB, with DNA gyrase: induction of DNA cleavage and blocking of transcription. *Journal of molecular biology* **273**, 826–839 (1997).
15. Hurley, J. M., Cruz, J. W., Ouyang, M. & Woychik, N. A. Bacterial toxin RelE mediates frequent codon-independent mRNA cleavage from the 5′ end of coding regions *in vivo*. *The Journal of biological chemistry* **286**, 14770–14778, doi:10.1074/jbc.M110.108969 (2011).
16. Hurley, J. M. & Woychik, N. A. Bacterial toxin HigB associates with ribosomes and mediates translation-dependent mRNA cleavage at A-rich sites. *The Journal of biological chemistry* **284**, 18605–18613, doi:10.1074/jbc.M109.008763 (2009).
17. Lopes, A. P. *et al.* VapC from the leptospiral VapBC toxin-antitoxin module displays ribonuclease activity on the initiator tRNA. *PloS one* **9**, e101678, doi:10.1371/journal.pone.0101678 (2014).
18. Munoz-Gomez, A. J., Santos-Sierra, S., Berzal-Herranz, A., Lemonnier, M. & Diaz-Orejas, R. Insights into the specificity of RNA cleavage by the Escherichia coli MazF toxin. *FEBS letters* **567**, 316–320, doi:10.1016/j.febslet.2004.05.005 (2004).
19. Pedersen, K. *et al.* The bacterial toxin RelE displays codon-specific cleavage of mRNAs in the ribosomal A site. *Cell* **112**, 131–140 (2003).

20. Gerdes, K. Toxin-antitoxin modules may regulate synthesis of macromolecules during nutritional stress. *Journal of bacteriology* **182**, 561–572 (2000).
21. Lewis, K. Persister cells. *Annual review of microbiology* **64**, 357–372 (2010).
22. Vazquez-Laslop, N., Lee, H. & Neyfakh, A. A. Increased persistence in Escherichia coli caused by controlled expression of toxins or other unrelated proteins. *Journal of bacteriology* **188**, 3494–3497, doi:10.1128/JB.188.10.3494-3497.2006 (2006).
23. Amitai, S., Yassin, Y. & Engelberg-Kulka, H. MazF-mediated cell death in Escherichia coli: a point of no return. *Journal of bacteriology* **186**, 8295–8300 (2004).
24. Jensen, R. B. & Gerdes, K. Programmed cell death in bacteria: proteic plasmid stabilization systems. *Molecular microbiology* **17**, 205–210 (1995).
25. Yarmolinsky, M. B. Programmed cell death in bacterial populations. *Science* **267**, 836–837 (1995).
26. Pandey, D. P. & Gerdes, K. Toxin-antitoxin loci are highly abundant in free-living but lost from host-associated prokaryotes. *Nucleic acids research* **33**, 966–976, doi:10.1093/nar/gki201 (2005).
27. Ramage, H. R., Connolly, L. E. & Cox, J. S. Comprehensive functional analysis of Mycobacterium tuberculosis toxin-antitoxin systems: implications for pathogenesis, stress responses, and evolution. *PLoS genetics* **5**, e1000767, doi:10.1371/journal.pgen.1000767 (2009).
28. Sala, A., Bordes, P. & Genevaux, P. Multiple toxin-antitoxin systems in Mycobacterium tuberculosis. *Toxins* **6**, 1002–1020, doi:10.3390/toxins6031002 (2014).
29. Fivian-Hughes, A. S. & Davis, E. O. Analyzing the regulatory role of the HigA antitoxin within Mycobacterium tuberculosis. *Journal of bacteriology* **192**, 4348–4356 (2010).
30. Gupta, A. Killing activity and rescue function of genome-wide toxin-antitoxin loci of Mycobacterium tuberculosis. *FEMS microbiology letters* **290**, 45–53, doi:10.1111/j.1574-6968.2008.01400.x (2009).
31. Korch, S. B., Contreras, H. & Clark-Curtiss, J. E. Three Mycobacterium tuberculosis Rel toxin-antitoxin modules inhibit mycobacterial growth and are expressed in infected human macrophages. *Journal of bacteriology* **191**, 1618–1630, doi:10.1128/JB.01318-08 (2009).
32. Korch, S. B., Malhotra, V., Contreras, H. & Clark-Curtiss, J. E. The Mycobacterium tuberculosis relBE toxin:antitoxin genes are stress-responsive modules that regulate growth through translation inhibition. *J Microbiol* **53**, 783–795, doi:10.1007/s12275-015-5333-8 (2015).
33. Miallau, L. *et al*. Structure and proposed activity of a member of the VapBC family of toxin-antitoxin systems. VapBC-5 from Mycobacterium tuberculosis. *The Journal of biological chemistry* **284**, 276–283 (2009).
34. Schifano, J. M. *et al*. Mycobacterial toxin MazF-mt6 inhibits translation through cleavage of 23S rRNA at the ribosomal A site. *Proceedings of the National Academy of Sciences of the United States of America* **110**, 8501–8506, doi:10.1073/pnas.1222031110 (2013).
35. Sharp, J. D. *et al*. Growth and translation inhibition through sequence-specific RNA binding by Mycobacterium tuberculosis VapC toxin. *The Journal of biological chemistry* **287**, 12835–12847, doi:10.1074/jbc.M112.340109 (2012).
36. Singh, R., Barry, C. E. 3rd & Boshoff, H. I. The three RelE homologs of Mycobacterium tuberculosis have individual, drug-specific effects on bacterial antibiotic tolerance. *Journal of bacteriology* **192**, 1279–1291, doi:10.1128/JB.01285-09 (2010).
37. Yang, M., Gao, C., Wang, Y., Zhang, H. & He, Z. G. Characterization of the interaction and cross-regulation of three Mycobacterium tuberculosis RelBE modules. *PloS one* **5**, e10672 (2010).
38. Zhu, L. *et al*. The mRNA interferases, MazF-mt3 and MazF-mt7 from Mycobacterium tuberculosis target unique pentad sequences in single-stranded RNA. *Molecular microbiology* **69**, 559–569, doi:10.1111/j.1365-2958.2008.06284.x (2008).
39. Zhu, L. *et al*. Characterization of mRNA interferases from Mycobacterium tuberculosis. *The Journal of biological chemistry* **281**, 18638–18643, doi:10.1074/jbc.M512693200 (2006).
40. Dahl, J. L. *et al*. The role of RelMtb-mediated adaptation to stationary phase in long-term persistence of Mycobacterium tuberculosis in mice. *Proceedings of the National Academy of Sciences of the United States of America* **100**, 10026–10031, doi:10.1073/pnas.1631248100 (2003).
41. Demidenok, O. I., Kaprelyants, A. S. & Goncharenko, A. V. Toxin-antitoxin vapBC locus participates in formation of the dormant state in Mycobacterium smegmatis. *FEMS microbiology letters* **352**, 69–77, doi:10.1111/1574-6968.12380 (2014).
42. Tiwari, P. *et al*. MazF ribonucleases promote Mycobacterium tuberculosis drug tolerance and virulence in guinea pigs. *Nature communications* **6**, 6059, doi:10.1038/ncomms7059 (2015).
43. Ahidjo, B. A. *et al*. VapC toxins from Mycobacterium tuberculosis are ribonucleases that differentially inhibit growth and are neutralized by cognate VapB antitoxins. *PloS one* **6**, e21738, doi:10.1371/journal.pone.0021738 (2011).
44. Venkataraman, B., Vasudevan, M. & Gupta, A. A new microarray platform for whole-genome expression profiling of Mycobacterium tuberculosis. *Journal of microbiological methods* **97**, 34–43, doi:10.1016/j.mimet.2013.12.009 (2014).
45. Boshoff, H. I. *et al*. The transcriptional responses of Mycobacterium tuberculosis to inhibitors of metabolism: novel insights into drug mechanisms of action. *The Journal of biological chemistry* **279**, 40174–40184, doi:10.1074/jbc.M406796200 (2004).
46. Morris, R. P. *et al*. Ancestral antibiotic resistance in Mycobacterium tuberculosis. *Proceedings of the National Academy of Sciences of the United States of America* **102**, 12200–12205, doi:10.1073/pnas.0505446102 (2005).
47. Betts, J. C., Lukey, P. T., Robb, L. C., McAdam, R. A. & Duncan, K. Evaluation of a nutrient starvation model of Mycobacterium tuberculosis persistence by gene and protein expression profiling. *Molecular microbiology* **43**, 717–731 (2002).
48. Brzozowska, I. & Zielenkiewicz, U. The ClpXP protease is responsible for the degradation of the Epsilon antidote to the Zeta toxin of the streptococcal pSM19035 plasmid. *The Journal of biological chemistry* **289**, 7514–7523, doi:10.1074/jbc.M113.519488 (2014).
49. Christensen, S. K. *et al*. Overproduction of the Lon protease triggers inhibition of translation in Escherichia coli: involvement of the yefM-yoeB toxin-antitoxin system. *Molecular microbiology* **51**, 1705–1717 (2004).
50. Donegan, N. P., Thompson, E. T., Fu, Z. & Cheung, A. L. Proteolytic regulation of toxin-antitoxin systems by ClpPC in Staphylococcus aureus. *Journal of bacteriology* **192**, 1416–1422, doi:10.1128/JB.00233-09 (2010).
51. Van Melderen, L., Bernard, P. & Couturier, M. Lon-dependent proteolysis of CcdA is the key control for activation of CcdB in plasmid-free segregant bacteria. *Molecular microbiology* **11**, 1151–1157 (1994).
52. Carroll, P., Brown, A. C., Hartridge, A. R. & Parish, T. Expression of Mycobacterium tuberculosis Rv1991c using an arabinose-inducible promoter demonstrates its role as a toxin. *FEMS microbiology letters* **274**, 73–82, doi:10.1111/j.1574-6968.2007.00842.x (2007).
53. Han, J. S. *et al*. Characterization of a chromosomal toxin-antitoxin, Rv1102c-Rv1103c system in Mycobacterium tuberculosis. *Biochemical and biophysical research communications* **400**, 293–298, doi:10.1016/j.bbrc.2010.08.023 (2010).
54. Huang, F. & He, Z. G. Characterization of an interplay between a Mycobacterium tuberculosis MazF homolog, Rv1495 and its sole DNA topoisomerase I. *Nucleic acids research* **38**, 8219–8230, doi:10.1093/nar/gkq737 (2010).
55. Robson, J., McKenzie, J. L., Cursons, R., Cook, G. M. & Arcus, V. L. The vapBC operon from Mycobacterium smegmatis is an autoregulated toxin-antitoxin module that controls growth via inhibition of translation. *Journal of molecular biology* **390**, 353–367, doi:10.1016/j.jmb.2009.05.006 (2009).
56. Schuessler, D. L. *et al*. Induced ectopic expression of HigB toxin in Mycobacterium tuberculosis results in growth inhibition, reduced abundance of a subset of mRNAs and cleavage of tmRNA. *Molecular microbiology* **90**, 195–207, doi:10.1111/mmi.12358 (2013).
57. Zhao, L. & Zhang, J. Biochemical characterization of a chromosomal toxin-antitoxin system in Mycobacterium tuberculosis. *FEBS letters* **582**, 710–714, doi:10.1016/j.febslet.2008.01.045 (2008).

58. Frampton, R., Aggio, R. B., Villas-Boas, S. G., Arcus, V. L. & Cook, G. M. Toxin-antitoxin systems of Mycobacterium smegmatis are essential for cell survival. *The Journal of biological chemistry* **287**, 5340–5356, doi:10.1074/jbc.M111.286856 (2012).
59. Albrethsen, J. *et al*. Proteomic profiling of Mycobacterium tuberculosis identifies nutrient-starvation-responsive toxin-antitoxin systems. *Molecular & cellular proteomics: MCP* **12**, 1180–1191, doi:10.1074/mcp.M112.018846 (2013).
60. McKenzie, J. L. *et al*. A VapBC toxin-antitoxin module is a posttranscriptional regulator of metabolic flux in mycobacteria. *Journal of bacteriology* **194**, 2189–2204, doi:10.1128/JB.06790-11 (2012).
61. Keren, I., Minami, S., Rubin, E. & Lewis, K. Characterization and transcriptome analysis of Mycobacterium tuberculosis persisters. *mBio* **2**, e00100–00111, doi:10.1128/mBio.00100-11 (2011).
62. Zhang, Y. *et al*. MazF cleaves cellular mRNAs specifically at ACA to block protein synthesis in Escherichia coli. *Molecular cell* **12**, 913–923 (2003).
63. Griffin, J. E. *et al*. High-resolution phenotypic profiling defines genes essential for mycobacterial growth and cholesterol catabolism. *PLoS pathogens* **7**, e1002251, doi:10.1371/journal.ppat.1002251 (2011).
64. Zhang, Y. J. *et al*. Global assessment of genomic regions required for growth in Mycobacterium tuberculosis. *PLoS pathogens* **8**, e1002946, doi:10.1371/journal.ppat.1002946 (2012).
65. DeJesus, M. A. *et al*. Comprehensive Essentiality Analysis of the Mycobacterium tuberculosis Genome via Saturating Transposon Mutagenesis. *mBio* **8**, doi:10.1128/mBio.02133-16 (2017).
66. Baga, M., Goransson, M., Normark, S. & Uhlin, B. E. Processed mRNA with differential stability in the regulation of *E. coli* pilin gene expression. *Cell* **52**, 197–206 (1988).
67. Belasco, J. G., Beatty, J. T., Adams, C. W., von Gabain, A. & Cohen, S. N. Differential expression of photosynthesis genes in R. capsulata results from segmental differences in stability within the polycistronic rxcA transcript. *Cell* **40**, 171–181 (1985).
68. McCarthy, J. E. Post-transcriptional control in the polycistronic operon environment: studies of the atp operon of Escherichia coli. *Molecular microbiology* **4**, 1233–1240 (1990).
69. Newbury, S. F., Smith, N. H., Robinson, E. C., Hiles, I. D. & Higgins, C. F. Stabilization of translationally active mRNA by prokaryotic REP sequences. *Cell* **48**, 297–310 (1987).
70. Nilsson, P. & Uhlin, B. E. Differential decay of a polycistronic Escherichia coli transcript is initiated by RNaseE-dependent endonucleolytic processing. *Molecular microbiology* **5**, 1791–1799 (1991).
71. Owolabi, J. B. & Rosen, B. P. Differential mRNA stability controls relative gene expression within the plasmid-encoded arsenical resistance operon. *Journal of bacteriology* **172**, 2367–2371 (1990).
72. Yu, X., Zheng, W., Bhat, S., Aquilina, J. A. & Zhang, R. Transcriptional and posttranscriptional regulation of Bacillus sp. CDB3 arsenic-resistance operon ars1. *PeerJ* **3**, e1230, doi:10.7717/peerj.1230 (2015).
73. Newbury, S. F., Smith, N. H. & Higgins, C. F. Differential mRNA stability controls relative gene expression within a polycistronic operon. *Cell* **51**, 1131–1143 (1987).
74. Desnoyers, G., Morissette, A., Prevost, K. & Masse, E. Small RNA-induced differential degradation of the polycistronic mRNA iscRSUA. *The EMBO journal* **28**, 1551–1561, doi:10.1038/emboj.2009.116 (2009).
75. Ruiz-Echevarria, M. J., de la Cueva, G. & Diaz-Orejas, R. Translational coupling and limited degradation of a polycistronic messenger modulate differential gene expression in the parD stability system of plasmid R1. *Molecular & general genetics: MGG* **248**, 599–609 (1995).
76. Baek, K. T. *et al*. beta-Lactam resistance in methicillin-resistant Staphylococcus aureus USA300 is increased by inactivation of the ClpXP protease. *Antimicrobial agents and chemotherapy* **58**, 4593–4603, doi:10.1128/AAC.02802-14 (2014).
77. Venkataraman, B., Gupta, N. & Gupta, A. A robust and efficient method for the isolation of DNA-free, pure and intact RNA from Mycobacterium tuberculosis. *Journal of microbiological methods* **93**, 198–202, doi:10.1016/j.mimet.2013.03.018 (2013).

Acknowledgements

This work was financially supported by Department of Biotechnology, Govt. of India. Processing of *M. tuberculosis* cultures was carried out in the BSL-3 facility at UDSC. Microarray experiments were performed at DBT-supported Genomic Facility at University of Delhi South Campus. Dr. V. K. Chaudhary and Dr. Vandana Malhotra are acknowledged for critical reading of the manuscript.

Author Contributions

A.G. conceived study, planned experiments, analyzed data and wrote the manuscript; V.B. grew *M. tuberculosis* cultures, isolated RNA and performed the microarray experiments; M.V. and K.B. performed bioinformatics analysis and representation of data for the manuscript in discussion with A.G.

Additional Information

Supplementary information accompanies this paper at doi:10.1038/s41598-017-06003-7

Competing Interests: The authors declare that they have no competing interests.

Publisher's note: Springer Nature remains neutral with regard to jurisdictional claims in published maps and institutional affiliations.